REVISED RESPONSE TO REQUEST FOR ADDITIONAL INFORMATION

APR1400 Design Certification

Korea Electric Power Corporation / Korea Hydro & Nuclear Power Co., LTD

Docket No. 52-046

RAI No.:	**208-8245**
SRP Section:	**03.08.03 – Concrete and Steel Internal Structures of Steel or Concrete Containments**
Application Section:	**03.08.03**
Date of RAI Issue:	**09/14/2015**

Question No. 03.08.03-1

10 CFR 50.55a and Appendix A to 10 CFR Part 50, General Design Criteria (GDC) 1, 2, 4, 16 and 50, provide the regulatory requirements for the design of structures including the in-containment refueling water storage tank (IRWST). Standard Review Plan (SRP) 3.8.3, Section II discusses the loads and load combinations normally applicable to internal concrete structures, particularly the IRWST, with emphasis on the extent of compliance with American Concrete Institute (ACI) 349-01, “Code Requirements for Nuclear Safety Related Concrete Structures,” with additional guidance provided in Regulatory Guide 1.142.

In DCD Tier 2, Section 3.8.3.1.8, “In-Containment Refueling Water Storage Tank,” the applicant stated that, “The design of the IRWST considers pressurization as a result of the reactor containment building systems design basis accident.” The applicant further stated in Appendix 3.8A, Section 3.8A.1.4.3.1.3, “Structural Design Summary,” report that, “The hydrodynamic pressure load, which is generated by the expulsion of air in the pilot-operated safety relief valve (POSRV) discharge, is applied to the wall and bottom slab of the IRWST through the two spargers.” The staff noted that additional information is needed in order to better understand the hydrodynamic pressure loads that are being considered for the analysis and design of the IRWST. Per 10 CFR 50.55a, Appendix A to 10 CFR Part 50, GDCs 1, 2, 4, 16 and 50; and SRP 3.8.3, the applicant is requested to provide additional information that fully describes the hydrodynamic pressure loads that are being considered in the analysis and design of the IRWST. The additional information should include a description, as to:

a. How the pressure transient (including the steady state portion) for a single sparger activation was developed (a figure of this load over time should be provided).

b. What cases of activation of the spargers may occur, i.e., one sparger alone, two spargers simultaneously, and/or some lag between the two activations.

c. How the total pressure transients on the walls and floor were developed based on the cases identified in item (b) above (a figure showing the pressure distributions on the walls and floor should be provided).

d. How the dynamic impact factor, discussed in DCD Section 3.8A.1.4.3.1.3, was determined, and explain why applying this as a static load is considered conservative.

Response – (Rev.1)

a. Pressure load on the IRWST due to actuation of POSRVs is governed by the air bubble dynamics during the discharge of air present in the piping. The largest hydrodynamic loads on the IRWST are dependent on the pressure and frequency of the air bubble formed during the air clearing phase.

TS

Based on the method developed by ABB-Atom and applied to the System 80+, scaling factors for the APR1400 design are developed as follows:

TS

Non-Proprietary

TS

TS

Upon actuation of the POSRVs, air in the lines is pressurized by the steam discharged from the RCS, forcing the water plug in the submerged pipe into the IRWST. Once the water in the pipe has cleared, the compressed air is released to the IRWST in the form of high pressure bubbles. These bubbles expand resulting in an outward acceleration of the surrounding IRWST water.

Air discharge is followed by the transport of saturated steam through the piping where it is discharged and condensed in the IRWST. The flow through the line continues, varying from saturated steam to two-phase to liquid, depending on thermodynamic conditions upstream and downstream of the SDS valves and in the transport piping.

The hydrodynamic loads during water and steady steam discharge phases are bounded by that of air discharge phase. The steam bubble oscillation issues can be neglected since discharged steam is fully condensed in the IRWST subcooled water.

Air clearing load test was carried out for the SKN3&4 nuclear power plant, the same reactor type as the APR1400, to verify the air clearing load results calculated using the ABB-Atom methodology that was applied to the System 80+. (The test “Unit Cell Sparger Test program” was conducted by KAERI (Korea Atomic Energy Research Institute) for the SKN3&4 IRWST and sparger design. [Ref. 1, Ref. 2 and Ref.3])

TS

b. The methodology for determining the pressure on the walls and floor is used for APR1400 the same as the System 80+.[Ref. 5]

The absolute pressure existing anywhere on the suppression pool boundary may be calculated from

$$P_a = P_{airspace} + \rho \frac{gh}{g_c} + \Delta P(r)$$

where

P_a : Pressure at any arbitrary point “a” on the suppression pool boundary (containment wall, basemat)

$P_{airspace}$: Pressure in the suppression pool airspace

$\frac{gh}{g_c}$: Pressure due to water head at point a

$\Delta P(r)$: Sparger air bubble differential pressure acting on wall at distance from the sparger center point

The attenuated bubble differential pressure $\Delta P(r)$ is calculated form the bubble differential pressure $\Delta P(r)$, time history relationships, and the relationship,

$$\Delta P_r = 2\Delta P_B \frac{r_o}{r} \quad \text{for} \quad r > 2r_O$$

$$\Delta P_r = \Delta P_B \quad \text{for} \quad r \le 2r_o$$

where

r_o : Maximum air bubble radius

r : Line of sight distance from sparger center point to the location of interest

Using basic trigonometry, distance, r_{ws}, from the sparger center point P_s (r_s, θ_s, z_s) to the interested point P_w (r_w, θ_w, z_w) in Figure 2 is

$$r_{ws} = \sqrt{r_w^2 + r_s^2 - 2r_w r_s \cos(\theta_w - \theta_s) + (z_w - z_s)^2}$$

To match boundary condition of atmospheric pressure at the pool surface, ΔP_r is assumed to decrease linearly to zero at the pool surface beginning from the value calculated at a position that is approximately 1/4 of the total sparger submergence depth. [Ref. 6]

Air bubble discharge loads from a particular sparger are considered to act only on the boundaries which can be "viewed" from the sparger bubble with direct line of sight as illustrated in Figure 2. To find the shade area, angle θ_{ws} on the line of the tangents to the sparger and inner wall can be expressed as

$$\theta_{ws} = \pm\left[\cos^{-1}\frac{r_{in}}{r_s} + \cos^{-1}\frac{r_{in}}{r_w}\right]$$

The shade regions between these two angles are not in direct line of sight of the depicted sparger discharge and, therefore, no load acts on these boundaries due to this sparger discharge.

For inner wall, substitute $r_w = r_{in}$ into above equation, then the angle becomes

$$\theta_{ws1} = \theta_{ws} = \pm\cos^{-1}\frac{r_{in}}{r_s}$$

and for outer wall, $r_w = r_{out}$, the angle becomes

$$\theta_{ws2} = \theta_{ws} = \pm\left[\cos^{-1}\frac{r_{in}}{r_s} + \cos^{-1}\frac{r_{in}}{r_{out}}\right]$$

For multiple valve actuation events, where more than one bubble exists in the pool, the foregoing calculation procedure is first utilized independently for each bubble. The combined load is then obtained by SRSS (Square Root of the Sum of Square) addition of these individual loads at the location of interest.

The combined pressure load considering activation of all POSRV spargers for APR1400 is expressed as follows:

$$\Delta P = \sqrt{\sum_{i=1}^{\text{No.of spargers}} \left(\Delta P_i\right)^2} \leq \Delta P_B$$

where,

- ΔP Resultant differential pressure above ambient at an interested point of the IRWST submerged wall boundary
- ΔP_i Differential pressure above ambient at an interested point of the IRWST submerged wall boundary due to i-*th* sparger (*i*=1….12 for APR1400)
- ΔP_B Maximum air bubble differential pressure above ambient (Source pressure)

The combined load is further limited to no greater than the maximum individual bubble source pressure(ΔP_B). The SRSS addition approach assumes all bubbles enter the pool simultaneously even though, in reality the bubbles will experience phase differences as a result of differences in key bubble formation parameters (e.g., valve actuation, valve opening time, line length, etc.). The SRSS technique, therefore, provides a simple representation of the effects of bubble phase differences on the combined load without requiring a detailed mechanistic model. The SRSS technique for combining loads from multiple bubbles is consistent with the conservative empirically based approach by which the individual bubble loads are calculated. [Ref. 6]

The POSRV discharge piping runs vertically down from the pressurizer and is connected to a common line near to the top head of the pressurizer and the two piping are finally routed to spargers submerged to the IRWST. Two pipes are located at Az. 90 degree (west direction) and Az. 180 degree (north direction) and are installed 6 spargers, respectively. Therefore, APR1400 uses12 spargers in the IRWST.

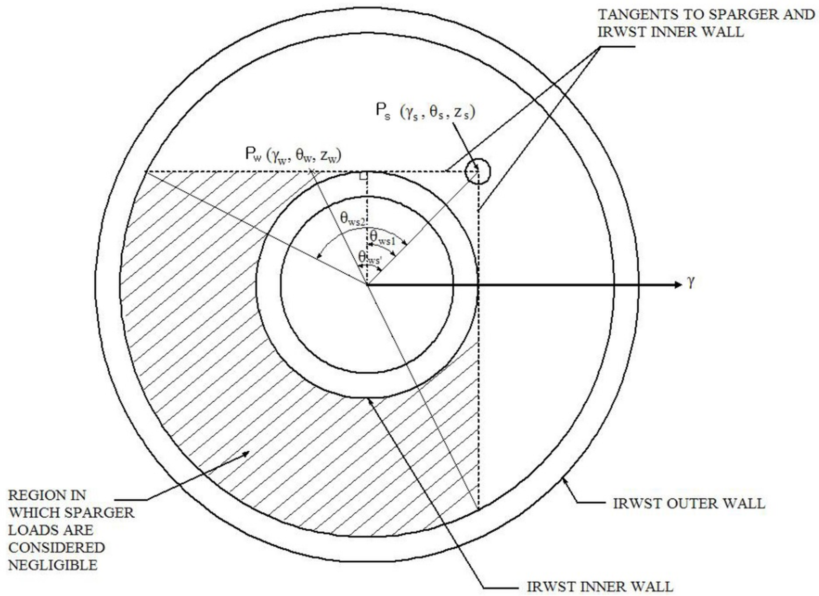

Figure 2. Line of Sight from Sparger

c. The hydrodynamic loads are the short transient pressure time histories at frequencies ranging from 4 Hz to 14 Hz. In the structural analysis for containment internal structure design, the maximum pressure value of the total pressure transient is conservatively obtained by applying a dynamic impact factor, and is considered as a static load. The maximum pressure value, which considers the dynamic impact factor, is distributed on the walls and floor in accordance with locations distances from spargers. A total of 12 spargers are located at Az. 90° (West Direction) and Az. 180° (North Direction), and the spatial distribution is expressed as a normalized factor. Figure 3 shows pressure distributions on the walls and the floor.

TS

d. The hydrodynamic load due to POSRV discharge is transient and normally the load experienced by the IRWST returns to ambient conditions in a short period of time. In the analytical procedure of fast load transients, the transient load can be simplified by introducing a dynamic load factor. It transforms a dynamic peak load into a static load with the same effect on the structure. In the case of an idealized triangle-shaped wave load, the dynamic load factor approaches its boundary limit of 2 (refer to Chapter 2 of "Introduction to Structural Dynamics", by John M. Biggs). Therefore, considering that the hydrodynamic load due to POSRV discharge is a short transient, and the shape of the pressure transient is a sine-curve (similar to triangle), the equivalent static load, with the application of a dynamic load factor, is conservative compared to the transient dynamic load.

References

[1] Korea Atomic Energy Research Institute (KAERI), "Air Clearing Load Tests and Analysis of Hydrodynamic Loads for SKN 3&4 Nuclear Power Plants", Test Report, January 2009. (Written in Korean)

[2] Development of Pressure Forcing Function for Estimating Air Clearing Load in IRWST for SKN 3&4 Nuclear Power Plants, January 2009. (Written in Korean)

[3] Korea Atomic Energy Research Institute (KAERI), "Air clearing pressure oscillation produced in a quenching tank by a prototype unit cell sparger of the APR14000", Research Paper in Science Direct, December 2007.

[4] “Experimental Investigation of Steam Vent Clearing Phenomena at system relief into a condensation pool of water”, Nilsson L., ABB-Atom Document, AE-RL-1630, 1975/9/17.

[5] Raytheon Nuclear. Inc., “Preliminary Assessment of Sparger Submergence Effects on KNGR IRWST Loads and Structural Analyses & Design”, Task Report, July 1996

[6] General Electric Company, “Mark II Containment Dynamic Forcing Functions Information Report”, NEDO-21061, Rev. 3 Class I, June, 1978.

Impact on DCD

DCD Tier2, Appendix 3.8A, Section 3.8A.1.4.3.1.3 will be revised, as indicated in the attached markup.

Impact on PRA

There is no impact on the PRA.

Impact on Technical Specifications

There is no impact on the Technical Specifications.

Impact on Technical/Topical/Environmental Reports

There is no impact on any Technical, Topical, or Environmental Report.

RAI 208-8245 - Question 03.08.03-1_Rev.1

c. SG compartment – SG blowdown nozzle

d. PZR compartment – PZR spray nozzle

e. PZR compartment – POSRV nozzle

f. PZR spray valve room – PZR spray line

Branch line pipe break (BLPB) loads are dynamic reactions caused by the combined effects of branch line nozzle reactions or thrust due to pipe break, jet impingement on RCS equipment, or subcompartment pressure effects on RCS equipment. The RCS support reactions due to BLPB are applied as nodal forces at the support locations.

12

The hydrodynamic pressure load, which is generated by the expulsion of air in the pilot-operated safety relief valve (POSRV) discharge, is applied to the wall and bottom slab of the IRWST through the ~~two~~ spargers. For the hydrodynamic pressure load, by multiplying the dynamic impact factor (DIF), the maximum pressure is conservatively considered as the static load in the analysis. In addition, the normalized factor is considered for the spatial distribution due to the location of spargers.

The seismic analysis for structures is performed using response spectrum analysis. A 7 percent damping ratio for reinforced concrete structures (SSE) and 3 percent damping ratio for the RCS model are used. In addition, the damping ratio for water in the IRWST or refueling pool is the same as that for reinforced concrete structures: the seismic response of water is only considered as impulsive (rigid) mode for structural analysis. Figure 3.8A-5 (a) and (c) show the in-structure response spectrum (ISRS) of the SSE level at El. 78 ft 0 in with 3 percent and 7 percent damping.

Three sections are selected in the PSW as critical sections. Each section is thinnest in the directions of north, south, and east. The design forces and moments for PSW critical sections are presented in the Table 3.8A-18. Table 3.8A-22 presents the margins of safety of rebar stress in the primary shield wall. The margin of safety is the ratio of allowable stress and actual stress.